Multiobjective optimization design of ultrahigh-head pump turbine runners with splitter blades

To cite this article: Zanao Hu *et al* 2019 *IOP Conf. Ser.: Earth Environ. Sci.* **240** 072036

IOP Conf. Series: Earth and Environmental Science **240** (2019) 072036 doi:10.1088/1755-1315/240/7/072036

Multiobjective optimization design of ultrahigh-head pump turbine runners with splitter blades

Zanao Hu1, Baoshan Zhu2*, Xiaobing Liu1, Zhe Ma2, Cheng Xue1

1 Key Laboratory of Fluid and Power Machinery, Ministry of education, Department of Energy and Power Engineering, Xihua University, Chengdu 610039, China. 2 State Key Laboratory of Hydroscienen and Engineering, Department of Energy and Power Engineering, Tsinghua University, Beijing 100084, China

*Author to whom correspondence should be addressed; Baoshan Zhu, Email: bszhu@mail.tsinghua.edu.cn

Abstract.The traditional design method, design-experiment-design, is time consuming and difficult. In the present paper, an efficiency design system for pump-turbine runners, the multiobjective optimization design system, which includes 3D inverse design, Computational Fluid Dynamics (CFD), Design Of Experiment (DOE), Radial Basis Function (RBF) and Multi Objective Genetic Algorithm (MOGA), is presented and then applied to design a scaled ultrahigh-head pump turbine runner. First, the control parameters, blade loading and the splitter work ratio, and the runner efficiencies under pump and turbine mode were selected as input variables and optimization objectives respectively. Then the DOE was applied to select the sample runners, and the CFD was used to predict the efficiencies of the sample runners under different modes. The relationship between input variables and objectives was built by RBF based on CFD results. Finally, the MOGA was applied to generate and search the good overall performance runners according to the relationship built by RBF. The results indicate that: the pump mode efficiency of preferred runner is increases by 0.34% and the turbine mode efficiency by 2.07% compared to the initial runner. With the improvement of efficiency, the pressure and streamline distribution are improved obviously. **Key words:** pump-turbine; multiobjective optimization; 3D inverse design; runner efficiency.

1. Introduction

With the rapid development of economic, the Pumped Storage Power Stations (PSPS) are becoming more and more important in the national power grid of China. As a result, the efficient operation of pump-turbine runner, which is the key component of energy conversion in PSPS, is of great significance for PSPS to improve the energy utilization. To promise the efficient operation of pump-turbine runners, how to design a good runner to fit the work condition is the most important. Generally, the pump-turbine runners are designed according to the pump work condition, and then verified in turbine mode[1]. Since the requirements for pump operation are difficult to meet, and when a pump works as a turbine, a relatively good performance can be maintained. However, the high efficiency operation zones under the pump mode and turbine mode don't coincide with each other, making it difficult to design a high efficiency runner under the two modes. Furthermore, the PSPS is developing towards high-head and large-capacity, bad cavitation characteristics and flow instability are the new changes for the design of pump-turbine runners [2]. The pump-turbine runners with splitter blades possess a wider high efficiency

zone and better cavitation characteristics, making it become a good choice for ultrahigh-head PSPS. However, the related research about how to development the ultrahigh-head runners with splitter blades is rare.

CFD technology has been widely used in the design and research of the pump-turbine runners [3][4]. In the traditional design method, the optimization design mainly depends on the internal flow analyses, providing by the CFD technology. This is considerably time consuming and requires intensive experience, since there is no directly relationship between the geometric control parameters and internal flow features. Therefore, more efficient and systematic approaches is necessary.

Recently, a multiobjective optimization strategy has been used to develop pump-turbine runners [2][5][6]. The advantage of the strategy is that the optimization process becomes organized, as the relationship between control parameters and optimization objects can be built by RBF model, and a compromise runner can be obtained by MOGA. In the present paper, the multiobjective optimization strategy was introduced at first. Thereafter, the strategy was applied to design a pump-turbine runner with splitter blades. Finally, numerical simulations were conducted to verify the optimization of the design system and analyses of the internal flows.

2. Multiobjective optimization design system

2.1. 3D inverse design

More and more scholars have accept the advantages of three-dimensional (3D) inverse design methods in the past 30 years[7][8].In the present paper, the commercial software TURBODesign for 3D inverse design was applied to parametrically describe the blade shapes. In TURBODesign, the blade shapes are controlled by the blade loading. For the incompressible potential flow, the relationship between blade loading and the blade pressure distribution can be expressed as follows[7][9][10].

$$p^{+} - p^{-} = \frac{2\pi}{B} \rho W_{mbl} \frac{\partial (r\overline{V}_{\theta})}{\partial m} \tag{1}$$

p^{+}, p^{-} are the pressure of pressure surface and suction surface respectively. B is the number of blades. For the pump-turbine runner with splitter blades, one blade contains one long blade and one short blade, W_{mbl} is the relative velocity on the blade surface, and $\partial (r\overline{V}_{\theta})/\partial m$ is blade loading.

2.2. CFD numerical simulation

The widely used commercial software ANSYS CFX15.0 was used to conduct the CFD analyses. ANSYS ICEM and TurboGrid were used for grid generation. All parts were structured grid. The extensively validated $RNG\ k\text{-}\varepsilon$ turbulence model was used for closing the N-S equations.

Figure 1 shows the computational domain, including spiral casing, stay vanes, guide vanes, runner, and draft tube. The wall of stationary and rotating parts was set for No-slip boundary condition, and the frozen rotor model was used for the interfaces between stationary and rotational components. For the pump mode, static pressure zero and mass flow rate were set as inlet and outlet boundary, respectively. For the turbine mode, the mass flow rate at rated condition was set at the inlet boundary and the static pressure zero was set as outlet boundary. The reference pressure of pump and turbine mode were both set as zero.

2.3. ISIGHT optimization platform

The design of experiment (DOE), the Radial Basis Function model (RBF), Multi Objective Genetic Algorithm (MOGA) were integrated together in ISIGHT platform. DOE was applied to choose sample runners from the design space scientifically, and the sample runners was then used to build RBF predict model. RBF is a type of neural network employing a hidden layer of radial units and an output layer of linear unites. RBF approximations are characterized by reasonably fast training and reasonably compact networks. It is useful in approximating a wide range of nonlinear spaces. Non-dominated Sorting Genetic Algorithm (NSGA-II), which is well-suited for highly non-linear and discontinuous design

spaces, was used for searching the compromise runners on the basis of the RBF model.

The first step of optimization was to select the input variables, and then the range of the input variables were determined by a large number of trial designs in TURBODesign5.2. After that, the DOE was used to select sample runners, equiprobably, randomly, and orthogonally. Each point can be designed to be a model runner by TURBODesign5.2. The ANSYS CFX15.0 was applied to estimate the efficiencies of the sample runners, and the RBF model between input variables and optimization targets was built on the basis of numerical simulation results. Finally, NSGA-II was applied to search the optimal solutions. The optimal result was based on the RBF model, and it could be obtained in a few minutes.

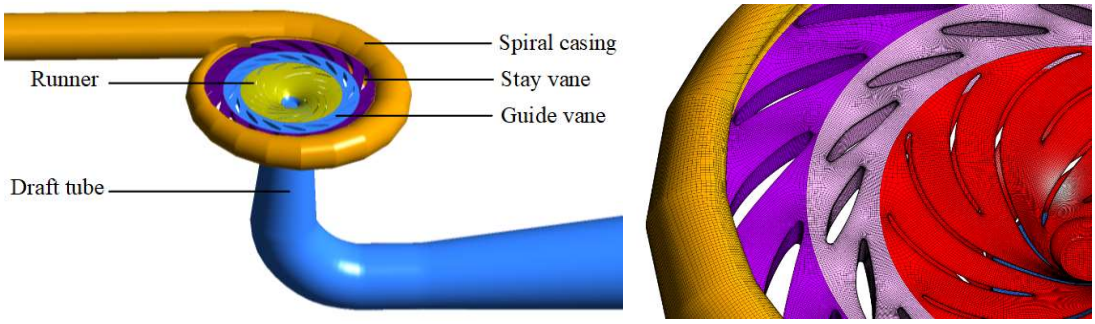

Figure 1. Computational domain.

3. Design of pump turbine runner with splitter

3.1. Optimization design parameters

The present paper is aim to obtain a high efficiency runner with splitter blades under both pump and turbine mode. In turbine mode, the rated head was H_r=659m , and the maximum and minimum net heads were $H_{\max} = 693.85$ m and $H_{\min} = 624.66$ m , respectively. In pump mode, the maximum and minimum heads were $H_{\max} = 712.46$ m and $H_{\min} = 652.11$ m , respectively. The rated capacity of the reversible synchronous motor was $P_r = 444.44$ MW and its rotational speed was $n_r = 500$ rpm

For the further research on the standard test rig, the scaled runners were designed. The design parameters are shown in Table1. The number of blades is twelve including six long blades and six short blades. Figure 2 shows the meridional shape of impeller, which were derived based on the centrifugal pump and one-dimension flow calculation. The control parameters are D_2 (high-pressure side diameter), b_2 (high-pressure side width), D_{1s} (low-pressure side shroud diameter), and D_{1h} (low-pressure side hub diameter). The values of these main parameters are given in Table 2.

3.2. Optimization process

In the present paper, only blade loading and the splitter work ratio were selected as input variables. The whole blade loading distributions are controlled by the blade loading given on hub and shroud streamlines. The blade loading between the hub and shroud was obtained from linear interrupt. As shown in Figure 3, each loading distribution curve includes three parts. Two parabolas locate at the head and tail, and a straight line in the middle. Each blade loading curve can be adjusted by the control parameters named DVRT, NC, ND, SLOP, which can be find in the Figure 3. Obviously, the blade loading needs 16 control parameters, in addition another parameter, splitter work ratio R_s, should be taken into consideration. So, there are 17 control parameters in total. The R_S is defined as Equation (2).

$$R_s = \frac{r\overline{V}^s_\theta}{r\overline{V}_\theta} \tag{2}$$

Table 1 Design parameters of mode pump-turbine.

Mode	$H_m(m)$	$Q_m(m^3/s)$	$N_m(rpm)$
Pump	59.40	0.28403	1200
Turbine	59.31	0.30529	1200

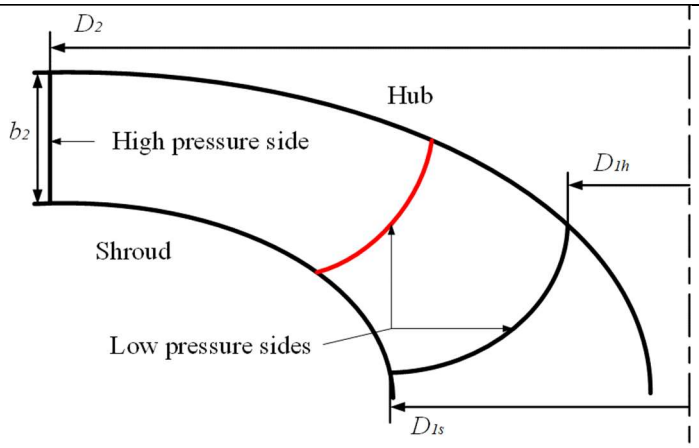

Figure 2. Meridional shape of blade.

Table 2. Control parameters of meridional blade shape.

Parameter	$D_{1h}(m)$	$D_{1s}(m)$	$B_2(m)$	$D_2(m)$
Value	0.132	0.250	0.042	0.132

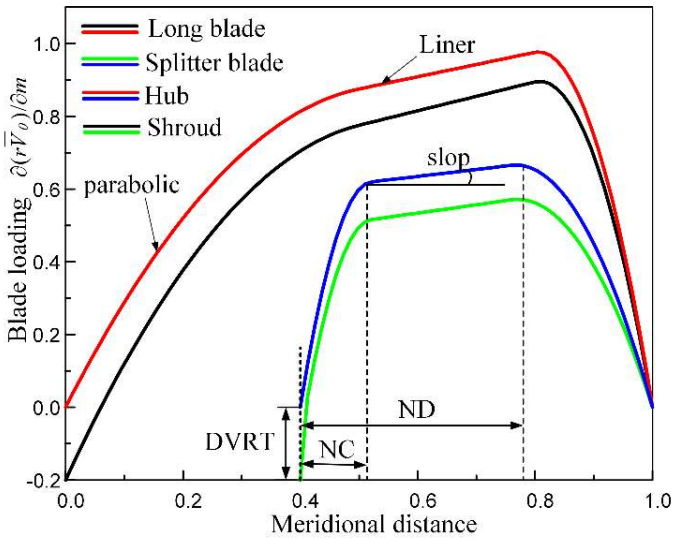

Figure 3. Blade loading.

As described above, the control parameters of the runners with splitters blades is much more than that of the normal runners [2]. This is not conductive to improving the accuracy of the RBF mode, and it will further impact the optimization result. To avoid that, extensive trial designs were conducted, and some unimportant parameters were fixed. The fixed valued were as follows. L-ND-h=0.8、L-ND-s=0.8、S-ND-h=0.8、S-ND-s=0.8、L-SLOP-h=0、L-SLOP-s=-0.3、S-SLOP-h=0.2、S-SLOP-s=0.2.In addition, the blade lean angle at the high-pressure side was θ=0°, and the splitter blades locate at the middle of long blades. The variation range of the other input variables were determined as shown in Table 3. The name of input variables was abbreviation. The first letter "L" means long blade, "S" means splitter. NC , ND were the intersection of the parabola and the straight line SLOP is the slop the straight line. The last letter "s" means shroud, "h" means hub. For example, L-ND-h=0.8 means the ND value of the hub of long blades.

Table 3. Variation range of input parameters.

Optimized Inputs	Parameters	Range
Blade loading	L-DVRT-h	-0.2~0.2
	L-DVRT-s	-0.2~0.2
	L-NC-h	0.05~0.8
	L-NC-s	0.05~0.8
	S-DVRT-h	-0.2~0.2
	S-DVRT-s	-0.2~0.2
	S-NC-h	0.05~0.8
	S-NC-s	0.05~0.8
Splitter work ratio	R_s	0.2~0.55

There is a one-to-one match between the combination of input parameters and model runners. The DOE was applied to determine the responsible combination of the variables, and the TURBODesign5.2 was then used to design the three-dimensional model of runners according to the combination of the variables. In total 60 runners were obtained in the present research. The TurboGide was used to gird generation for sample runners. To avoid the impact of mesh quality on numerical simulation results, the mesh independence test was carried out before the optimization, and the mesh number of the runners was finally determined to be 1050000 for each sample runner. In addition, the average y^+ for each sample runners was controlled under 100.

The efficiencies under pump mode and turbine mode at the design point were selected as optimization objects. Therefore, 120 times CFD numerical simulation were conducted to get the efficiencies under different mode.

The efficiencies under pump and turbine mode were calculated by in Equations (3) and (4), respectively.

$$\eta_{mp} = \frac{\rho g H_{mp} Q_{mp}}{M_{mp} \omega_{mp}} \tag{3}$$

$$\eta_{mT} = \frac{\rho g H_{mT} Q_{mT}}{M_{mT} \omega_{mT}} \tag{4}$$

ω_{mp} is the angular velocity under pump mode, ω_{mT} is the angular velocity under turbine mode, M_m is the momentum, which is calculated through the CFD analyses.

Based on numerical simulation results, the RBF mode was built. After that, the genetic algorithm （NSGA-II） was applied to generate and search the optimal runner.

3.3. Optimization result

Figure 4 shows the optimization results. Each point represents a model runner. There are 10000 different optimized runners, which are generated by NSGA-II based on RBF mode. The blue points are the Pareto optimum front, which is the optimum solution set of the optimization.

Three runners, marked by A1, A2, A3, were chosen from the Pareto optimum solution set for further research. Table 4 shows the performance comparisons calculated by CFD and estimated by RBF. The initial runner was also reported. Although there are some differences between RBF predict and CFD analyses, the performances estimated by the RBF model are reliable, and the maximum error is 0.19%. After comprehensive comparison, the final design was confirmed as runner A3. Compared to the baseline runner, the pump efficiency is increased by 0.34% and the turbine efficiency by about 2.07%.

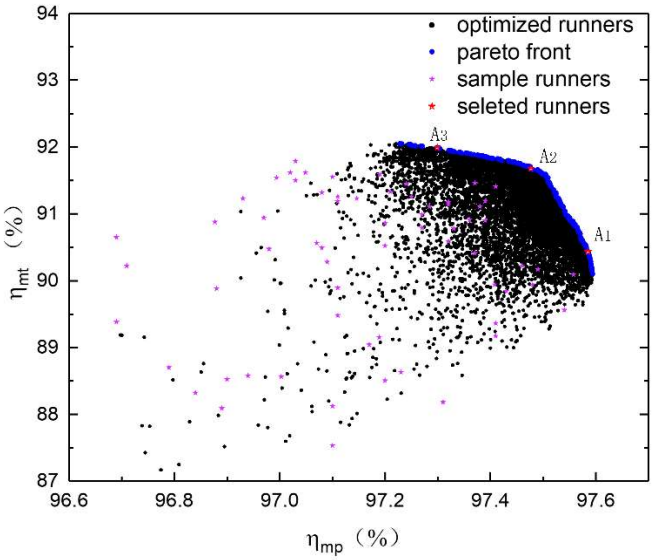

Figure 4. Optimization result.

Table 4. Optimization results

Runner	Mode	efficiency		Error
		RBF	CFD	
A_1	Pump	97.59	97.45	0.14%
	Turbine	90.43	90.33	0.11%
A_2	Pump	97.47	97.30	0.17%
	Turbine	91.68	91.62	0.07%
A_3	Pump	97.29	97.11	0.19%
	Turbine	91.99	91.89	0.11%
Initial runner	Pump	—	96.77	—
	Turbine	—	89.82	—

3.4. Result analysis

Figure 5 shows the difference of blade loading between the initial runner and the preferred runner A3. It is demonstrated that the blade loading distribution curve of the splitter blades is much higher after optimized. The R_s of the preferred runner and the initial runner is 0.549 and 0.220, respectively.

The difference of blade shape between the preferred runner and initial runner is shown in Figure 6. The wrap angle of preferred runner is much bigger than that of the initial runner. This contributes to increasing the efficiency under the turbine mode, according to the result as show in Table 4.

The impacts of control parameters on the runner efficiencies have been researched in this paper. According to Figure 7, the impacts of control parameters on pump mode efficiency are much smaller than those on turbine mode efficiency, and the variable that has the greatest impact on both pump and turbine mode efficiencies is proved to the splitter work ratio R_s.

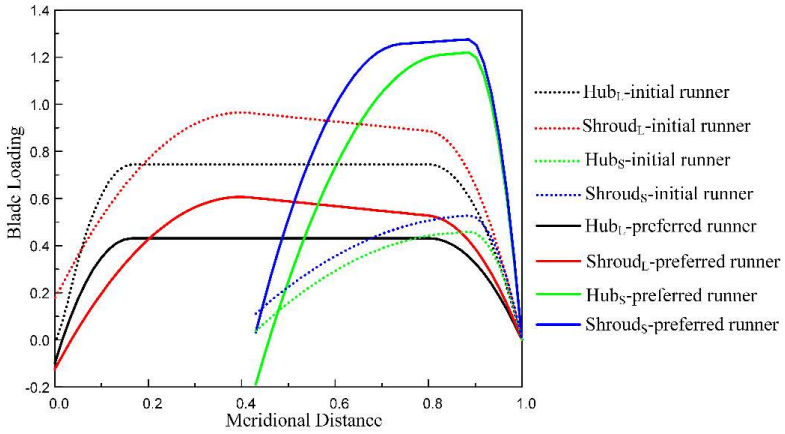

Figure 5. Blade loading distribution of the initial runner and preferred runner.

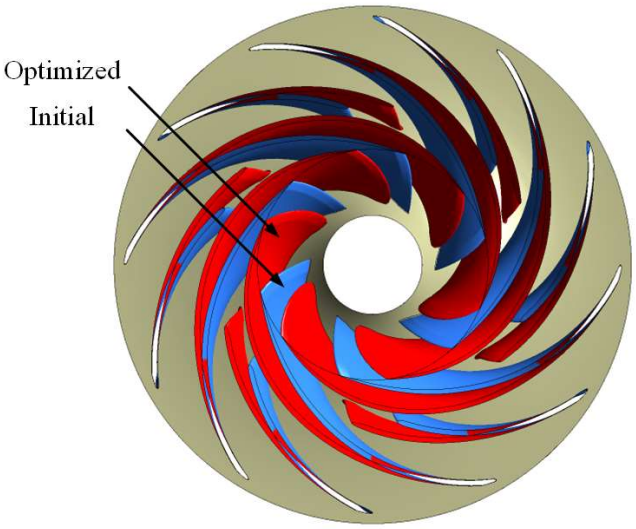

Figure 6. Comparison of blades.

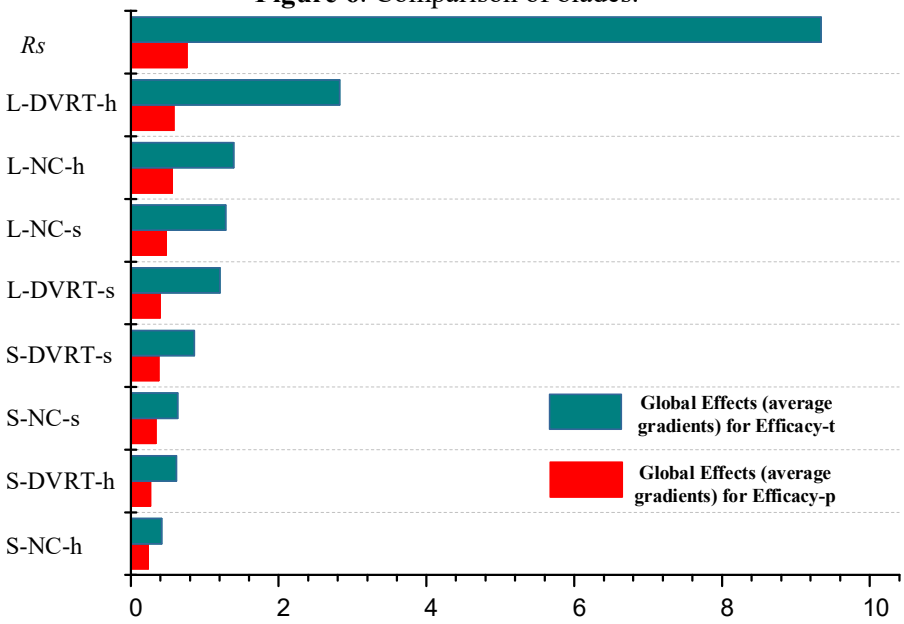

Figure 7. Global effects (average gradients) for runner.

To further research the impacts of R_s on the runner efficiencies, two more runners, B1 B2, have been designed by changing the R_s and keeping the rest of variables the same with the preferred runner. Thereafter, the numerical simulations have been applied to the two runners, and the results are shown in Table 5. Compared the runner A3 with the runner B1, with the R_s decreasing from 0.549 to 0.350, the pump and turbine efficiency decrease by 0.32% and 1.88%, respectively. While compared the initial runner with the runner A3, the pump efficiency is increased by 0.34% and the turbine efficiency by 2.07%. Obviously, the improvement of efficiencies is mainly attributed to the increase of R_s. Therefore, the larger R_s is recommended, when designing the runners with splitter blades.

Table 5. The impacts of R_s on efficiencies.

Runers	*Rs*	η_{mp} /100%	η_{mt} /100%
B1	0.350	96.79	90.01
B2	0.450	97.01	90.98
A3	0.549	97.11	91.89
Initial	0.220	96.77	89.82

The numerical simulations have been applied to study the flow feature of the initial runner and the preferred runner. Figure 8 shows the streamlines pictures and the pressure contours on the middle flow surface under the rated condition. The blade arrows in the Figure 8 a) b) show the specific flow direction under different mode. The sections of preferred runner are obviously smoother compare to that of the initial runner. As show in Figure 8 a), there is seriously flow separation at the high-pressure sides, and further develop into vertex in the middle channel under the turbine mode. The vortexes cause greatly hydraulic loss, and lead to low efficiency in turbine mode. The flow separation is improved obviously after optimization. As a result, the efficiency of turbine mode increases about 2%.

Under the pump mode, the phenomenon of flow separation is much better than that of turbine mode, as show in Figure 8 b). The flow separation is suppressed after optimization, making the pump efficiency increase slightly.

Figure 8 c) d) show the pressure contours under different mode. It is demonstrated that the pressure gradient of the preferred runner is uniform than that of the initial runner, and the variation of pressure gradient is mainly concentrated in the high-pressure side area in turbine mode. In addition, the low-pressure area of preferred runner is improved and the cavitation performance of the optimized runner is better theoretically.

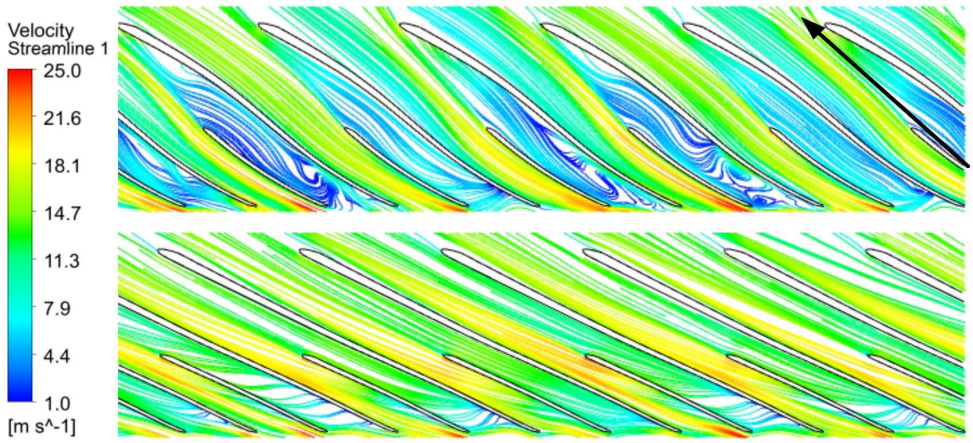

a)

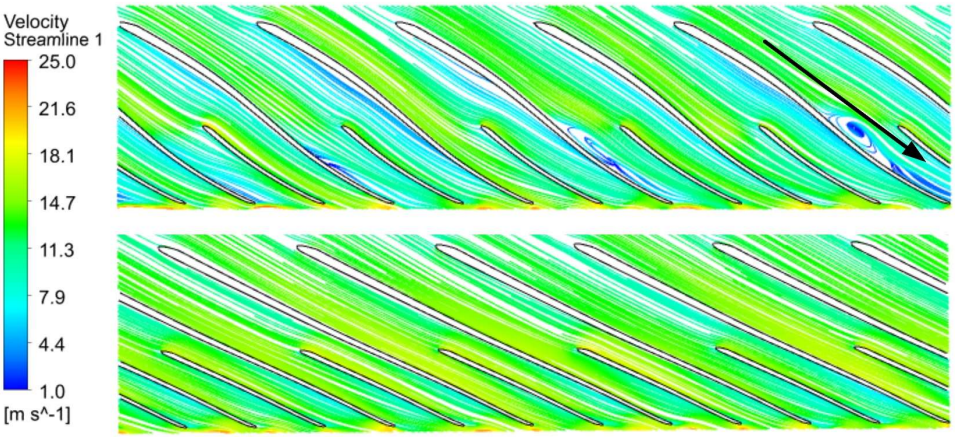

b)

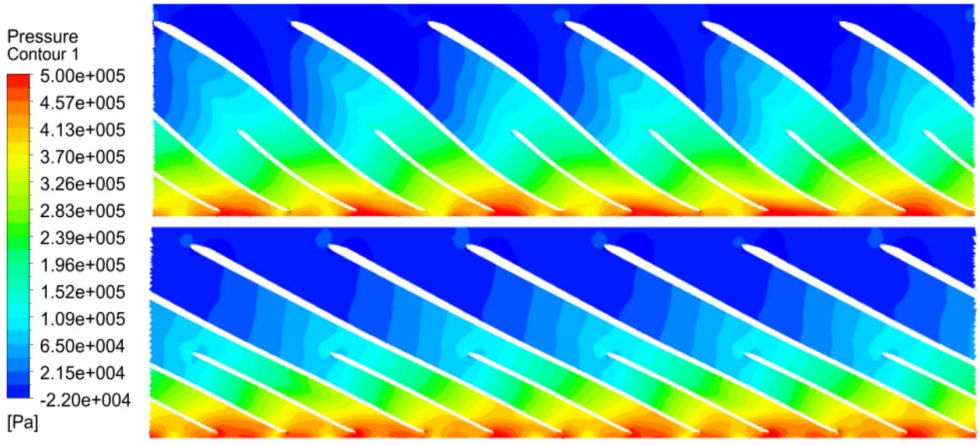

c)

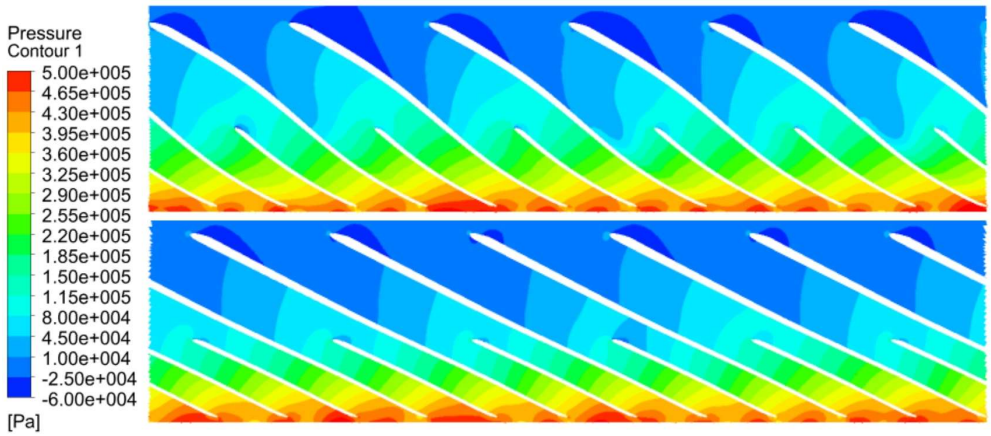

d)

Figure 8. a) Velocity streamlines of turbine mode, b) velocity streamlines of pump mode, c) pressure contours of turbine mode, d) pressure contours of pump mode (up initial, down preferred).

4. Conclusion

In the present paper, a multiobjective optimization design strategy, which combines the 3D inverse design, CFD, DOE, RBF, MOGA, is introduced at first, and it was then applied to design the pump-turbine runners with splitter blades. The results show that the larger splitter work ratio is benefitting to

improve the runner efficiencies. Compared to the initial runner, the pump efficiency is increased by 0.34% and the turbine efficiency by 2.07%. With the increases of efficiencies, the flow pattern and the pressure distribution of the preferred runner are improved obviously. These results provide a guideline for design ultrahigh-head pump-turbine runners with splitter blades.

References

[1] Chen C, Zhu B, Singh P M, and Choi Y D 2015 Design of a pump-turbine based on the 3d inverse design method. *Forum of the Korean Society for fluid machinery*. **18**(1), 20-28.

[2] Liu L, Zhu B, Bai L, Liu X and Zhao Y 2017 Parametric design of an ultrahigh-head pump-turbine runner based on multiobjective optimization. *Energies*, **10**(8), 1169.

[3] Schleicher W C and Oztekin A 2015 Hydraulic design and optimization of a modular pump-turbine runner. *Energy Conversion and Management*, **93**(9), 388-398.

[4] Kerschberger P and Gehrer A. Hydraulic development of high specific-speed pump-turbines by means of an inverse design method, numerical flow-simulation (CFD) and model testing 2010 *IOP Conference Series: Earth and Environmental Science*, 012039.

[5] Zhu B, Wang X, Tan L, Zhou D, Zhao Y and Cao S. 2015. Optimization design of a reversible pump–turbine runner with high efficiency and stability. *Renewable Energy*. **81**, 366-376.

[6] Wang X H, Zhu B S, Cao S L and Tan L 2013 Full 3-D viscous optimization design of a reversible pump turbine runner. *Materials Science and Engineering Conference Series*. **52** (2):66-71.

[7] Zangeneh M 2010 A compressible three-dimensional design method for radial and mixed flow turbomachinery blades. *International Journal for Numerical Methods in Fluids*. **13**(5). 599-624.

[8] Tan L, Cao S, Wang Y and Zhu B 2012 Direct and inverse iterative design method for centrifugal pump impellers. *Proceedings of the Institution of Mechanical Engineers Part A J. Power and Energy*. **226**(6). 764-775.

[9] Bonaiuti D 2009 On the coupling of inverse design and optimization techniques for the multiobjective, multipoint design of turbomachinery blades. *J. Turbomachinery*, **131**(2). 021014-021029.

[10] Zangeneh M, Goto A and Harada H 1998 On the design criteria for suppression of secondary flows in centrifugal and mixed flow impellers. *J. Turbomachinery*. **120**(4), 723-735.